NOAA TECHNICAL MEMORANDUM NWS ER-68

A COMPARISON AMONG VARIOUS THERMODYNAMIC PARAMETERS FOR THE PREDICTION OF CONVECTIVE ACTIVITY

Hugh M. Stone
National Weather Service Eastern Region
Garden City, New York

Scientific Services Division
Eastern Region Headquarters
April 1985

U.S. DEPARTMENT OF COMMERCE / National Oceanic and Atmospheric Administration / National Weather Service

NOAA TECHNICAL MEMORANDA
National Weather Service, Eastern Region Subseries

The National Weather Service Eastern Region (ER) Subseries provides an informal medium for the documentation and quick dissemination of results not appropriate, or not yet ready for formal publications. The series is used to report on work in progress, to describe technical procedures and practices, or to relate progress to a limited audience. These Technical Memoranda will report on investigations devoted primarily to regional and local problems of interest mainly to ER personnel, and hence will not be widely distributed.

Papers 1 to 22 are in the former series, ESSA Technical Memoranda, Eastern Region Technical Memoranda (ERTM); papers 23 to 37 are in the former series, ESSA Technical Memoranda, Weather Bureau Technical Memoranda (WBTM). Beginning with 38, the papers are now part of the series, NOAA Technical Memoranda NWS.

Papers 1 to 22 are available from the National Weather Service Eastern Region, Scientific Services Division, 585 Stewart Avenue, Garden City, N.Y. 11530. Beginning with 23, the papers are available from the National Technical Information Service, U.S. Department of Commerce, Sills Bldg., 5285 Port Royal Road, Springfield, Va. 22151. Prices vary for paper copy; $2.25 microfiche. Order by accession number shown in parentheses at end of each entry.

ESSA Technical Memoranda

ERTM 1 Local Uses of Vorticity Prognoses in Weather Prediction. Carlos R. Dunn April 1965
ERTM 2 Application of the Barotropic Vorticity Prognostic Field to the Surface Forecast Problem. Silvio G. Simplicio. July 1965
ERTM 3 A Technique for Deriving an Objective Precipitation Forecast Scheme for Columbus, Ohio. Robert Kuessner. September 1965
ERTM 4 Stepwise Procedures for Developing Objective Aids for Forecasting the Probability of Precipitation. Carlos R. Dunn. November 1965
ERTM 5 A Comparative Verification of 300 mb. Winds and Temperatures Based on NMC Computer Products Before and After Manual Processing. Silvio G. Simplicio. March 1966
ERTM 6 Evaluation of OFDEV Technical Note No. 17. Richard M. DeAngelis. March 1966
ERTM 7 Verification of Probability of Forecasts at Hartford, Connecticut, for the Period 1963-1965. Robert B. Wassall. March 1966
ERTM 8 Forest-Fire Pollution Episode in West Virginia November 8-12, 1964. Robert O. Weedfall. April 1966
ERTM 9 The Utilization of Radar in Meso-Scale Synoptic Analysis and Forecasting. Jerry D. Hill. March 1966
ERTM 10 Preliminary Evaluation of Probability of Precipitation Experiment. Carlos R. Dunn. May 1966
ERTM 11 Final Report. A Comparative Verification of 300 mb. Winds and Temperatures Based on NMC Computer Products Before and After Manual Processing. Silvio G. Simplicio. May 1966
ERTM 12 Summary of Scientific Services Division Development Work in Sub-Synoptic Scale Analysis and Prediction - Fiscal Year 1966. Fred L. Zuckerberg.
ERTM 13 A Survey of the Role of Non-Adiabatic Heating and Cooling in Relation of the Development of Mid-Latitude Synoptic Systems. Constantine Zois. July 1966
ERTM 14 The Forecasting of Extratropical Onshore Gales at the Virginia Capes. Glen V. Sachse. August 1966
ERTM 15 Solar Radiation and Clover Temperatures. Alex J. Kish. September 1966
ERTM 16 The Effects of Dams, Reservoirs and Levees on River Forecasting. Richard M. Greening. September 1966
ERTM 17 Use of Reflectivity Measurements and Reflectivity Profiles for Determining Severe Storms. Robert E. Hamilton. October 1966
ERTM 18 Procedure for Developing a Nomograph for Use in Forecasting Phenological Events from Growing Degree Days. John C. Purvis and Milton Brown. December 1966
ERTM 19 Snowfall Statistics for Williamsport, Pa. Jack Hummel. January 1967
ERTM 20 Forecasting Maturity Date of Snap Beans in South Carolina. Alex J. Kish. March 1967
ERTM 21 New England Coastal Fog. Richard Fay. April 1967
ERTM 22 Rainfall Probability at Five Stations Near Pickens, South Carolina, 1957-1963. John C. Purvis. April 1967.
WBTM ER 23 A Study of the Effect of Sea Surface Temperature on the Areal Distribution of Radar Detected Precipitation Over the South Carolina Coastal Waters. Edward Paquet. June 1967 (PB-180-612)
WBTM ER 24 An Example of Radar as a Tool in Forecasting Tidal Flooding. Edward P. Johnson. August 1967 (PB-180-613)
WBTM ER 25 Average Mixing Depths and Transport Wind Speeds over Eastern United States in 1965. Marvin E. Miller. August 1967 (PB-180-614)
WBTM ER 26 The Sleet Bright Band. Donald Marier. October 1967 (PB-180-615)
WBTM ER 27 A Study of Areas of Maximun Echo Tops in the Washington, D.C. Area During the Spring and Fall Months. Marie D. Fellechner. April 1968 (PB-179-339)
WBTM ER 28 Washington Metopolitan Area Precipitation and Temperature Patterns. C.A. Woollum and N.L. Canfield. June 1968 (PB-179-340)
WBTM ER 29 Climatological Regime of Rainfall Associated with Hurricanes after Landfall. Robert W. Schoner. June 1968 (PB-179-341)
WBTM ER 30 Monthly Precipitation - Amount Probabilities for Selected Stations in Virginia. M.H. Bailey. June 1968 (PB-179-342)
WBTM ER 31 A Study of the Areal Distribution of Radar Detected Precipitation at Charleston, S.C. S.K. Parrish and M.A. Lopez. October 1968 (PB-180-480)
WBTM ER 32 The Meteorological and Hydrological Aspects of the May 1968 New Jersey Floods. Albert S. Kachic and William Long. February 1969 (Revised July 1970) (PB-194-222)
WBTM ER 33 A Climatology of Weather that Affects Prescribed Burning Operations at Columbia, South Carolina. S.E. Wasserman and J.D. Kanupp. December 1968 (COM-71-00194)
WBTM ER 34 A Review of Use of Radar in Detection of Tornadoes and Hail. R.E. Hamilton. December 1969 (PB-188-315)
WBTM ER 35 Objective Forecasts of Precipitation Using PE Model Output. Stanley E. Wasserman. July 1970 (PB-193-378)
WBTM ER 36 Summary of Radar Echoes in 1967 Near Buffalo, N.Y. Richard K. Sheffield. September 1970 (COM-71-00310)
WBTM ER 37 Objective Mesoscale Temperature Forecasts. Joseph P. Sobel. September 1970 (COM-71-0074)

NOAA Technical Memoranda NWS

NWS ER 38 Use of Primitive Equation Model Output to Forecast Winter Precipitation in the Northeast Coastal Sections of the United States. Stanley E. Wasserman and Harvey Rosenblum. December 1970 (COM-71-00138)
NWS ER 39 A Preliminary Climatology of Air Quality in Ohio. Marvin E. Miller. January 1971 (COM-71-00204)
NWS ER 40 Use of Detailed Radar Intensity Data in Mesoscale Surface Analysis. Robert E. Hamilton. March 1971 (COM-71-00573)
NWS ER 41 A Relationship Between Snow Accumulation and Snow Intensity as Determined from Visibility. Stanley E. Wasserman and Daniel J. Monte May 1971 (COM-71-00763)
NWS ER 42 A Case Study of Radar Determined Rainfall as Compared to Rain Gage Measurements. Martin Ross. July 1971 (COM-71-00897)
NWS ER 43 Snow Squalls in the Lee of Lake Erie and Lake Ontario. Jerry D. Hill. August 1971 (COM-72-00959)
NWS ER 44 Forecasting Precipitation Type at Greer, South Carolina. John C. Purvis. December 1971 (COM-72-10332)
NWS ER 45 Forecasting Type of Precipitation. Stanley E. Wasserman. January 1972 (COM-72-10316)
NWS ER 46 An Objective Method of Forecasting Summertime Thunderstorms. John F. Townsend and Russell J. Younkin. May 1972 (COM-72-10765)
NWS ER 47 An Objective Method of Preparing Cloud Cover Forecasts. James R. Sims. August 1972 (COM-72-11382)
NWS ER 48 Accuracy of Automated Temperature Forecasts for Philadelphia as Related to Sky Condition and Wind Direction. Robert B. Wassall. September 1972 (COM-72-11473)
NWS ER 49 A Procedure for Improving National Meteorologiacal Center Objective Precipitation Forecasts. Joseph A. Ronco, Jr. November 1972 (COM-73-10132)
NWS ER 50 PEATMOS Probability of Precipitation Forecasts as an Aid in Predicting Precipitation Amounts. Stanley E. Wasserman. December 1972 (COM-73-10243)
NWS ER 51 Frequency and Intensity of Freezing Rain/Drizzle in Ohio. Marvin E. Miller. February 1973 (COM-73-10570)
NWS ER 52 Forecast and Warning Utilization of Radar Remote Facsimile Data. Robert E. Hamilton. July 1973 (COM-73-11275)
NWS ER 53 Summary of 1969 and 1970 Public Severe Thunderstorm and Tornado Watches Within the National Weather Service, Eastern Region. Marvin E. Miller and Lewis H. Ramey. October 1973 (COM-74-10160)
NWS ER 54 A Procedure for Improving National Meteorological Center Objective Precipitation Forecasts - Winter Season. Joseph A. Ronco, Jr. November 1973 (COM-74-10200)
NWS ER 55 Cause and Prediction of Beach Erosion. Stanley E. Wasserman and David B. Gilhousen. December 1973 (COM-74-10036)
NWS ER 56 Biometeorological Factors Affecting the Development and Spread of Plant Diseases. V. J. Valli. July 1974 (COM-74-11625/AS)
NWS ER 57 Heavy Fall and Winter Rain In The Carolina Mountains. David B. Gilhousen. October 1974 (COM-74-11761/AS)
NWS ER 58 An Analysis of Forecasters' Propensities In Maximum/Minimum Temperature Forecasts. I. Randy Racer. November 1974 (COM-75-10063/AS)

(Continued On Inside Rear Cover)

NOAA TECHNICAL MEMORANDUM NWS ER-68

A COMPARISON AMONG VARIOUS THERMODYNAMIC PARAMETERS FOR THE PREDICTION OF CONVECTIVE ACTIVITY

Hugh M. Stone
National Weather Service Eastern Region
Garden City, New York

Scientific Services Division
Eastern Region Headquarters
April 1985

A COMPARISON AMONG VARIOUS THERMODYNAMIC PARAMETERS FOR THE PREDICTION OF CONVECTIVE ACTIVITY

I. Introduction

The development of convection requires a sufficient moisture source, unstable air, and a triggering mechanism. We shall be concerned here only with the effect of atmospheric instability on convection. A variety of different stability indices are now in use, the most recent of these being the energy indices, EI1 and EI2 (Stone 1983, 1984 a, b).

The AFOS applications program RANP (Stone, 1984a) computes several of these indices along with some other thermodynamic parameters, which were considered to be possibly useful in forecasting convection. A statistical evaluation of the performance of some of these parameters as predictors of both convection and severe weather is presented herein. The VIP level reported in the MDR portion of radar observations was used as a measure of the intensity of convection.

The performance of the lifted, K, Showalter, EI1 and EI2 stability indices was investigated. The EI1 index is an integration of energy areas terminating at the 400 mb level and the EI2 index terminates at the equilibrium level. EI2 is not always defined, since it requires some positive energy area in the troposphere to locate the equilibrium level, and this may not exist under very stable conditions.

The EI1 and EI2 indices are both computed with an entrainment process (Austin, 1948), which mixes environmental air into the ascending parcel. An entrainment rate is used that increases the mass of the parcel by 60 percent over a 500 mb ascent. An experiment was performed using several different entrainment rates for the energy indices EI1 and EI2. Correlations with ensuing convective activity showed that the 60 percent entrainment usually gave the best results.

Another parameter computed in conjunction with the energy index is called ETCCL. The convective condensation level (CCL) is required for this parameter and may be determined on a thermodynamic diagram by the intersection of the mean mixing ratio line, representative of the lowest 100 mb of the sounding, with the temperature trace (Haltiner and Martin, 1957). ETCCL is defined as the energy area between the dry adiabat through the CCL and the temperature trace from the CCL to the surface. ETCCL based on the 1200 GMT raob is an estimate of the amount of solar heating required to initiate afternoon convection. ETCCL based on the 0000GMT raob may be interpreted as a measure of low level stability inhibiting surface based convection.

An additional parameter not usually considered is based on the concept of potential instability. If wet bulb potential temperature decreases with height through an atmospheric layer and that layer is lifted until saturation occurs, then the lapse rate through the layer will be unstable for saturated air. A crude measure of potential instability called DMAX[1] was defined as the depth (in millibars) of the deepest potentially unstable layer in the atmosphere. Of course, this neglects the amount of lift required to achieve saturation in any part of the layer, which determines whether potential instability can be converted to real instability. Despite its crudity, DMAX was tested as a possible predictor of convective activity.

In addition to the investigation of the performance of the various stability indices, correlations between the heights of radar tops and occurrences of severe weather were also examined. Correlation coefficients were computed for radar top heights above ground level, above tropopause level, and above equilibrium level.

II. Data Collection

Data were collected over a six month period between April and September 1984. The following nine stations were selected at which radiosonde and radar observations were both available:

PWM	Portland, ME
ACY	Atlantic City, NJ
HAT	Cape Hatteras, NC
CHS	Charleston, SC
BUF	Buffalo, NY
PIT	Pittsburgh, PA
BNA	Nashville, TN
AHN	Athens, GA
AYS	Waycross, GA

Only data that were operationally available on the AFOS circuit were used. No attempt was made to retrieve data that were missing for any reason. Significant level radiosonde data were used in the computation of the various stability indices and equilibrium level. Tropopause and standard level heights were extracted from the mandatory level radiosonde data. Tropopause and equilibrium levels were converted from pressure units to height units by interpolations using the height of the standard pressure levels. Data collection was done for both the 1200 GMT and 0000 GMT synoptic times.

Radar MDR data were collected for all twelve hours following the synoptic times with a count being made of the various radar VIP levels in each MDR box within 125 nautical miles of the station for the first six hour period

1. DMAX does not explicitly appear in the output from the RANP program, but is computed from the "Deepest Pot. Unstable Layer" on bottom line of the WRKTPA product.

following the synoptic time and the second six hour period. Counts were made for three overlapping categories of VIP levels: VIP ≥ 1, VIP ≥ 3, and VIP ≥ 5. Radar VIP levels of 3 or more are generally indicative of thunderstorms. In addition, the maximum radar top reported within each six hour period was recorded. All twelve radar observations following the synoptic time were required to be available; if one or more were missing, that station was excluded from the statistics for that hour. This strict requirement caused the loss of approximately one third of the potential data sample, but was considered necessary to assure the quality of the remaining sample.

A count of severe weather events for each six hour period within 125 nautical miles of each of the nine stations was also made. This information was obtained from the "Tornado and Severe Thunderstorm Reports - Preliminary List" compiled by the National Severe Storms Forecast Center in Kansas City, Mo., and distributed daily as AFOS product CCCSTADTS. This is a preliminary list with incomplete data. Therefore, the count we have recorded is usually smaller than the actual number of severe weather events. This must be considered in the interpretation of the statistics to be discussed later.

III. Results

To assess the relationship between the various stability indices and the occurrence or non-occurrence of the three categories of VIP levels, point biserial correlation coefficients were computed for each of the six hour periods. The point biserial correlation coefficient measures the relationship between a continuous variable, e.g. energy index, and a binary variable, e.g. occurrence or non-occurrence of a particular VIP level. Since the bulk of convective activity in the eastern United States occurs between 1800 GMT and 0600 GMT, only those correlation coefficients for the two six hour periods, 1800 GMT to 2400 GMT and 0000 GMT to 0600 GMT, will be discussed. The restriction to these two time periods is essential when point biserial correlation coefficients for severe weather occurrences are considered; this is because severe weather occurrences outside of this time period are so rare that the correlation coefficients are unreliable.

Correlation coefficients for the 1800-2400 GMT time period are shown in Table 1. The first three columns show the correlation between the stability indices computed from 1200 GMT raob data and various radar VIP levels which were observed 6 to 12 hours later. It is seen that the EI1 index has a somewhat higher correlation with the VIP levels than any of the other indices. VIP levels of 3 or more usually indicate thunderstorms and this is the VIP level which is best correlated with all the stability indices. At this VIP level, EI1 is best correlated, with lifted index second best, and K index the worst of the standard indices. ETCCL and DMAX both have relatively low correlations -.4440 and .3845, respectively. A multiple correlation coefficient was then computed combining EI1, ETCCL, and DMAX with a resulting coefficient of .6724. This is an insignificant improvement of approximately .01 over the simple coefficient of .6621 for EI1 alone.

Correlation coefficients do not tell the full story of the performance of the various stability parameters. To investigate further, histograms of relative frequency of occurrence of VIP level 3 for each of the six stability parameters are shown in figure 1. Intervals of histograms are chosen so that at least 10 cases are contained in each interval; some intervals are wider than others so that a sample of at least 10 is represented. The lower number at the top of each bar is the total number of cases in that interval and the upper number is the number of cases where VIP level 3 or greater was observed. For reliability a large number of cases in each interval is desired. Stability values that are exactly on an interval ending point are counted in the interval to the left, i.e., in Fig. 1.B. lifted index interval -3 to 0 actually includes -2, -1, and 0 and a lifted index of -3 would be counted in the -6 to -3 interval.

The EI1 index based on 1200 GMT data had the best correlation coefficient .6621 and seems to also have the most useful histogram shown in fig. 1.A. From the data sample of 373 cases, 32 cases had EI1 greater than 40 and all 32 observed radar VIP 3 or more between 1800 GMT and 2400 GMT, a 100 percent relative frequency. For EI1 in the range of 0 to 40, the relative frequency was approximately 89 percent. For stable situations with EI1 of -80 or less, VIP level 3 was observed about 9 percent of the time.

Lifted index (Fig. 1.B) provided a good threshold for the non-occurrence of VIP3; it was not observed with index more than 18. However, the upper threshold for occurrence of VIP3 was not quite as good with a relative frequency of 93 percent for lifted index -3 or lower and 91 percent for the 0 to -3 interval.

The Showalter index (Fig. 1.C) shows a 94 percent frequency of occurrence for values of the index -3 or lower, while the K index (Fig. 1.D) was most reliable at values greater than 32 with a 91 percent frequency of occurrence of VIP level 3 or greater. The histogram of ETCCL (Fig. 1.E) was particularly poor with 259 cases, 69 percent of the sample, clustered in the 0 to 40 interval with a relative frequency of 68 percent. Likewise, the histogram of DMAX (Fig. 1.F) provided little useful information with most of sample having relative frequencies in the 40 to 70 percent range.

The various stability parameters based on the 0000 GMT raob data were correlated with occurrence of radar VIP levels 1, 3, and 5 during the period 0000 GMT to 0600 GMT. This time period was chosen since very little convective activity occurs in the Eastern Region after 0600 GMT. The correlation coefficients for this group of data are shown in Table 2. It is seen that EI1 again has the better correlation for VIP levels 3 and 5 compared to the other stability indices. For VIP level 1, the K index is best with a correlation of .5341. The K index was also better than lifted or Showalter index for the VIP level 1 correlations shown in Table 1. The K index is sensitive to mid level (700 mb) moisture, while the lifted and Showalter indices are effected only by the moisture of the parcel and not the environmental moisture. This is probably the reason for the better correlation with the lower VIP levels 1 and 2, since a deep moist layer in the atmosphere is more likely to result in many convective elements with low radar VIP levels, rather than a few convective elements with higher VIP levels. The EI1 index is also sensitive to environmental moisture, because of the entrainment process used in the computation, and it was found that correlation with VIP levels of 1 or greater was increased by increasing the entrainment rate. However, for correlation with VIP level 3 or greater, the original entrainment rate was best.

The correlation coefficients of Table 2 (0000 GMT) are generally lower than the coefficients of Table 1 (1200 GMT data). This is probably due to the fact that stability indices from the 1200 GMT data are representative of the pre-convective state of the atmosphere, while indices from the 0000 GMT data frequently have already been influenced by ongoing convective activity. It is fortunate that better correlations are obtained from the 1200 GMT data, since the need to evaluate stability is more important at that time rather than in the evening after convection has usually begun. With ongoing convection, techniques are available for short range extrapolation of storms and the location of new convection may be estimated by determining outflow boundary intersections and so forth. The role of the stability index in forecasting is of lesser importance in the evening.

Histograms of the relative frequency of occurrence of radar VIP level 3 or greater for the various stability indices based on 0000 GMT data are shown in Figure 2. Comparing them with the histograms based on the 1200 GMT data of Figure 1, it is apparent that the 0000 GMT histograms are less useful. For example, the threshold of greater than 40 for the EI1 index (Fig. 2A) establishes a relative frequency of only 82 percent. None of the the other indices are any better, and the poor performance of ETCCL and DMAX are again confirmed for this time period. Multiple correlation coefficients combining EI1, ETCCL and DMAX again revealed no significant improvement over the correlation of EI1 by itself.

Correlation of severe weather occurrences with various values of the stability indices were also computed and are shown in the last column of Table 1 (1200 GMT data) and Table 2 (0000 GMT data). We recorded only 35 incidents of severe weather in the time period 1800 GMT - 2400 GMT and 15 incidents in the period 0000 GMT - 0600 GMT. The more rare an occurrence of some phenomenum, the more difficult it becomes to establish good correlation coefficients with a predictor. This is readily apparent in both Tables 1 and 2, as the correlation coefficients for all the stability indices declines steadily going from column 2 to column 4; VIP ≥ 5 is more difficult to correlate than VIP ≥ 3 and the severe weather correlations are worst of all.

For the period 1800 GMT to 2400 GMT using stability indices from 1200 GMT, the best correlation of severe weather was with the Showalter index, R = -.2097, which was just slightly better than EI1 and lifted index. All of the indices have poor correlations and the worst are ETCCL and DMAX. The same results were generally found using the indices from 0000 GMT. In this case, EI1 was the slightly better index, but essentially the same as the lifted, K, and Showalter index.

Relative frequency histograms for severe weather occurrences in the 1800 GMT - 2400 GMT time period are shown in Figure 3. They are not very useful. When EI1 exceeds 40 the frequency of occurrence of severe weather is 25 percent; the same threshold provided a 100 percent occurrence of VIP level 3 or more (Fig. 1A). The development of severe weather is strongly dependent on the proper moisture stratification and appropriate dynamic forcing. Some degree of instability is also required, but it is clearly not the controlling factor.

The best correlations of severe weather were with radar top heights. This is shown in Table 1 (time period 1800 GMT - 2400 GMT) and Table 2 (time period 0000 GMT - 0600 GMT). Radar tops have traditionally been compared to tropopause height to assess their potential for severe weather (Darrah, 1978). Tropopause penetration has been shown to be a better predictor of severe weather west of the Appalachians and not well related east of the Appalachians. More recently it has been suggested that the equilibrium level is the physically meaningful level for assessing the severity of storms (Burgess and Davies-Jones, 1979, Doswell, et al., 1982). The correlation coefficients as shown in Table 1 and Table 2 do not confirm the value of the equilibrium level as a reference point for radar tops in forecasting severe weather. For the 1800 GMT - 2400 GMT period, height of radar tops above equilibrium level had a correlation of .2504 with severe weather occurrence, while height of radar tops above tropopause had a correlation of .3590 and correlation with radar tops alone was virtually the same .3580. Table 2 for the 0000 GMT - 0600 GMT time period shows a similar relationship but lower correlations.

Histograms of relative frequency of occurrence of severe weather for radar tops above equilibrium level, above tropopause level, and above ground level are shown in Figures 4A, 4B, and 4C respectively. The afternoon time period is on the left side of the figure and the evening on the right. Figure 4 shows a 29 percent frequency of severe weather during the 1800 GMT - 2400 GMT time period when radar tops exceed the equilibrium level by more than 27000 feet and 51 percent frequency when radar tops exceed tropopause level by more than 7000 feet. For the 0000 GMT - 0600 GMT period there is similarly a better relationship to tropopause level. These results are somewhat surprising, since theoretically the equilibrium level should be the relevant level for assessing the strength of convection. Our data sample for severe weather is relatively small and may possibly be non-representative. Figure 4A does show that nearly all severe weather occurrences are accompanied by radar tops exceeding the equilibrium level, but there are many more cases where tops exceed equilibrium level and severe weather is not observed.

We have not yet considered the performance of the EI2 index. EI2 as mentioned previously is frequently not defined when the atmosphere is very stable. To compute correlation coefficients for EI2, all cases of missing EI2 were removed from the sample, which resulted in a decrease in sample size from 373 cases down to 234 cases for the 1200 GMT data, and a decrease from 501 to 360 cases for the 0000 GMT data. The comparison of correlation coefficients for EI1 and EI2 are shown in Table 3 for the 1800 GMT - 2400 GMT time period. The correlations of EI2 with both radar VIP ≥ 3 and severe weather are much worse than the EI1 correlations. The correlations of EI2 are similary poor for the 0000 GMT - 0600 GMT time period. The corresponding histograms were compared and it was found that EI2 provided no information that was not already apparent from the EI1 histograms.

The poor performance of EI2 is probably related to the vertical distribution of positive and negative areas encountered during the computation of the indices. Recall that the vertical integration of energy areas for the EI1 index arbitrarily terminates at the 400 mb level, but the EI2 integration terminates at the equilibrium level, which may be either above or below the 400 mb level. With a high equilibrium level it is possible to get a fairly large value of EI2, with most of the positive energy area above the 400 mb level, and a rather low value of EI1. If the positive energy area is too high in the atmosphere with a large negative area below it, this is not conducive to the development of convection, since a rising parcel will probably not be able to reach the positive area. The EI1 index is apparently more sensitive to stability in the lower atmosphere and is thereby able to differentiate more accurately between the convective and non-convective situations.

IV. Conclusions

Stability indices based on the 1200 GMT raob data are better correlated with the development of afternoon convection than the 0000 GMT stability indices with evening convection. This is fortunate, since the assessment of stability prior to the beginning of convection is more important in forecasting than stability measurements after the convection has already begun, which is usually the case by 0000 GMT.

The correlation coefficients of Table 1 and the frequency histograms of Figure 1, both indicate that the EI1 index is somewhat better than the lifted, K, or Showalter index in forecasting afternoon convective activity. This is in accordance with experience in using the various indices in daily forecast situations. On many days the choice of stability index is immaterial, indications are similar for all of them, but on some days the EI1 index points the correct way, while one or more of the others is misleading.

The use of the parameters ETCCL and DMAX in forecasting does not seem to be justified. Their performance singly is inferior to any of the other indices and when used in combination with the EI1 index there is no significant increase in performance as determined by multiple correlation computations. Likewise, the EI2 index does not appear to be a useful predictor of either convection or severe weather. Correlation coefficients are much lower for EI2 than any of the other stability indices; the problem appears to be lack of ability to discern the stable situations.

The performance of all the stability indices is poor with regard to severe weather prediction. As mentioned before, rare events are difficult to predict, and severe weather is relatively rare compared to the common thunderstorm. Severe weather is more dependent on appropriate dynamical forcing than other types of convection, so the role of instability, although important, is not the dominant factor.

The best correlation with severe weather was obtained from radar tops or the excess of radar tops over tropopause level. This is shown by the data in Tables 1 and 2 and the histograms of relative frequency in Figure 4. The importance of the equilibrium level for assessing the intensity of convection is not demonstrated by our data sample, which is relatively small and possibly non-representative.

The entire set of statistics presented in this report should be considered tentative, especially those involving severe weather, because of the relatively small sample size. Despite this deficiency, we believe the results are essentially correct, based on day to day forecast experience. The histograms of Figure 1A,B,C,D should be useful to the forecaster, since they give an idea of the probability of occurrence of thunderstorms for various ranges of the different stability indices. The left side of Figure 4 relating the occurrence of afternoon severe weather to radar tops may also be useful, but must be used with caution due to the small data sample previously mentioned.

V. References

Austin, J.M., 1948: A Note on Cumulus Growth in a Nonsaturated Environment, Journal of Meteorology, 5, 103-107.

Burgess, D.W. and R.P. Davies-Jones, 1979: Unusual Tornadic Storms in Eastern Oklahoma on 5 December 1975. Mon. Wea. Rev., 107, 451-457.

Darrah, R.P., 1978: On the Relationship of Severe Weather to Radar Tops. Mon. Wea. Rev., 106, 1332-1339.

Doswell, C.A., J.T. Schaefer, D.W. McCann, T.W. Schlatter, and H.B. Wobus, 1982: Thermodynamic Analysis Procedures at the National Severe Storms Forecast Center, Preprints, 9th Conf. Weather Forecasting and Analysis, Amer. Meteor. Soc., Seattle, 304-309.

Haltiner, G.J. and F.L. Martin, 1957: Dynamical and Physical Meteorology, McGraw-Hill Book Co., pp. 57-63.

Stone, H.M., 1983: Stability Analysis Program, NOAA Eastern Region Computer Programs and Problems NWS ERCP-No. 9, National Weather Service, Garden City, NY.

Stone, H.M., 1984a: RANP: Stability Analysis Plot Program, NOAA Eastern Region Computer Programs and Problems NWS ERCP-No. 16, National Weather Service, Garden City, NY.

Stone, H.M., 1984b: The Energy Index for Stability, Preprints, 10th Conf. Weather Forecasting and Analysis, Amer. Meteor. Soc., Clearwater Beach, Fl, 550-554.

Table 1. Point biserial correlation coefficients for 1800 GMT to 2400 GMT. Stability indices, equilibrium level and tropopause height at 1200 GMT. Radar tops from 1800-2400 GMT. Sample size 373. Best correlations are underlined.

	VIP≥1	VIP≥3	VIP≥5	Severe Weather
Energy Index 1	<u>.5309</u>	<u>.6621</u>	<u>.4860</u>	.2079
Lifted Index	-.4437	-.6372	-.4843	-.2058
K Index	.5231	.5415	.4035	.1438
Showalter Index	-.4944	-.6071	-.4705	-.2097
ETCCL	-.3630	-.4440	-.3075	-.1197
DMAX	.2835	.3845	.2871	.1224
Radar Tops - Equilibrium Level				.2504
Radar Tops - Tropopause				<u>.3590</u>
Radar Tops				.3580

Table 2. Point biserial correlation coefficients for 0000 GMT to 0600 GMT. Stability indices, equilibrium level and tropopause height at 0000 GMT. Radar tops from 0000-0600 GMT. Sample size 501. Best correlations are underlined.

	VIP≥1	VIP≥3	VIP≥5	Severe Weather
Energy Index 1	.4927	<u>.5712</u>	<u>.4053</u>	.1590
Lifted Index	-.3670	-.4991	-.3637	-.1432
K Index	<u>.5341</u>	.5077	.3277	.1509
Showalter Index	-.4571	-.4920	-.3467	-.1455
ETCCL	-.3926	-.3237	-.2047	-.0712
DMAX	.1713	.2868	.2458	.0922
Radar Tops - Equilibrium Level				.1270
Radar Tops - Tropopause				.2373
Radar Tops				<u>.2642</u>

Table 3. Point biserial correlation coefficients for 1800 GMT to 2400 GMT. Stability indices from 1200 GMT raobs. Sample size reduced to 234 cases to eliminate missing EI2 values.

	VIP≥3	Severe Weather
EI1	.5654	.1569
EI2	.3220	.0651

VIP≥3 (18Z-24Z)

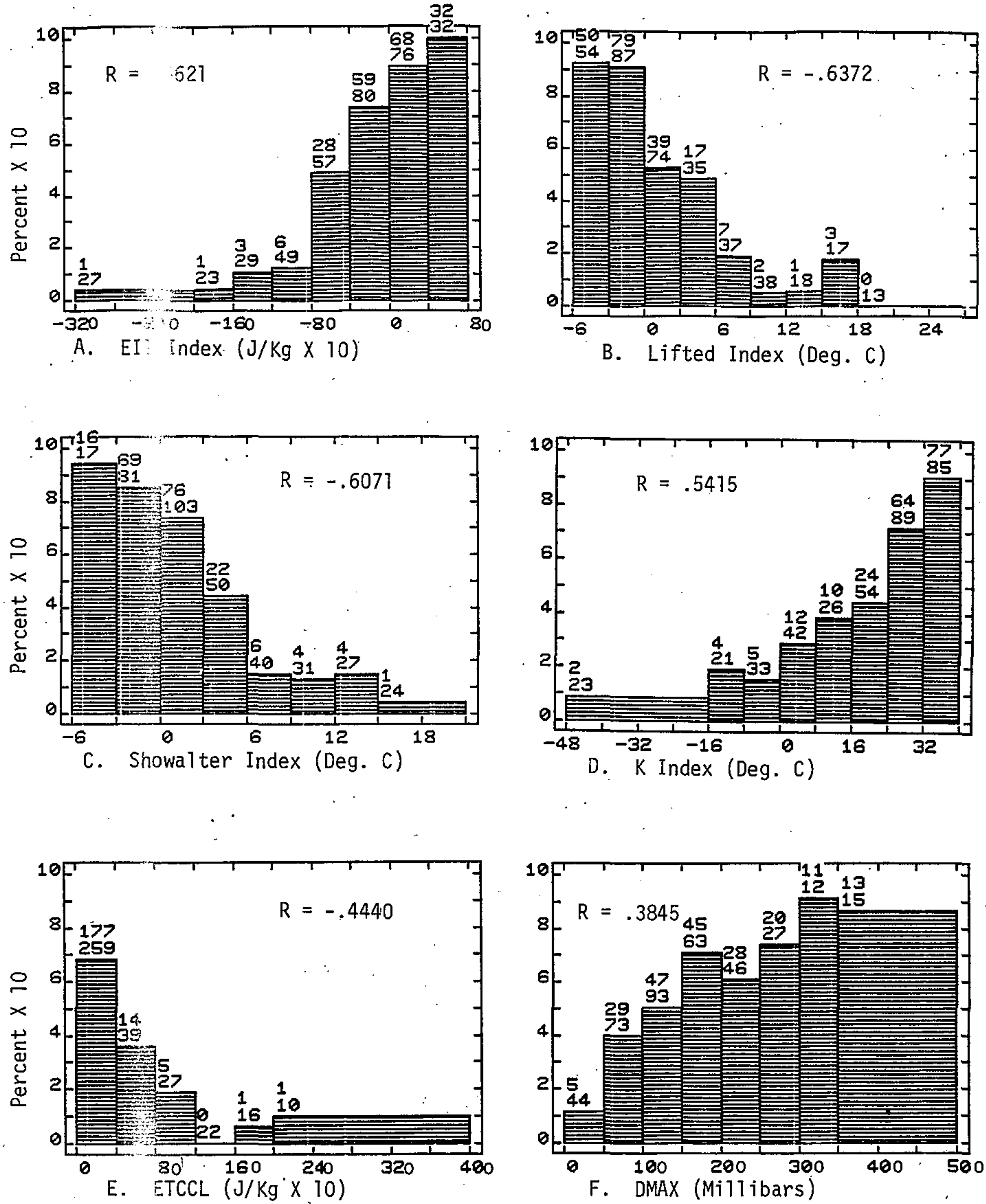

Fig. [illegible]. Histograms of relative frequency of occurrence of VIP level 3 or greater (between 18Z-24Z) for various stability parameters computed from 1200GMT raob data. Top number above each bar is number of occurrences of VIP>3; bottom number is number of cases in the interval. Total number of cases is 373. Any interval containing less than 10 cases was expanded and combined with an adjacent interval. Correlation coefficient (R) is given for each histogram.

VIP≥3 (00Z-06Z)

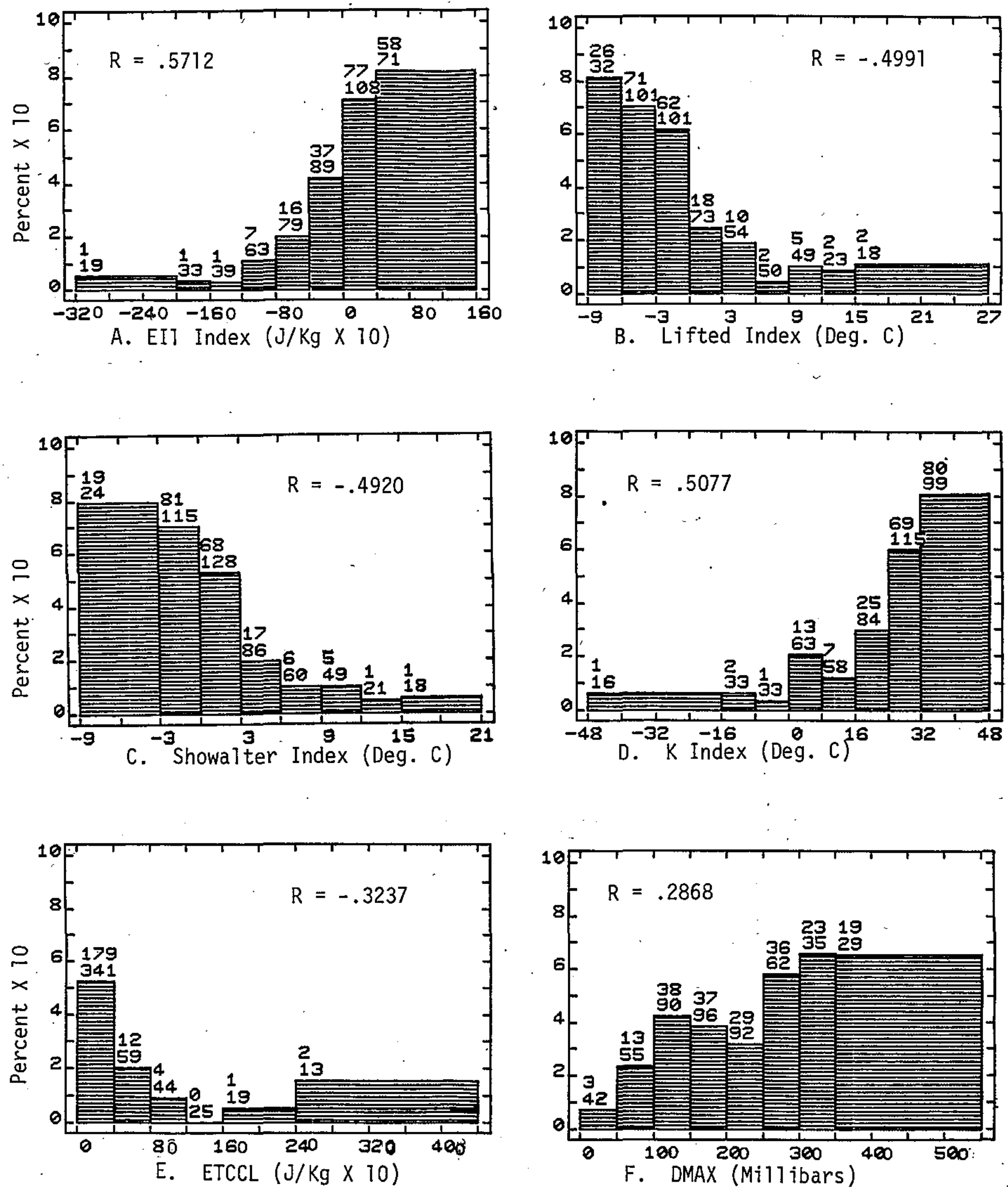

Fig. 2. Histograms of relative frequency of occurrence of VIP level 3 or greater (between 00Z-06Z) for various stability parameters computed from 0000GMT raob data. Total number of cases is 501.

SEVERE WEATHER (18Z-24Z)

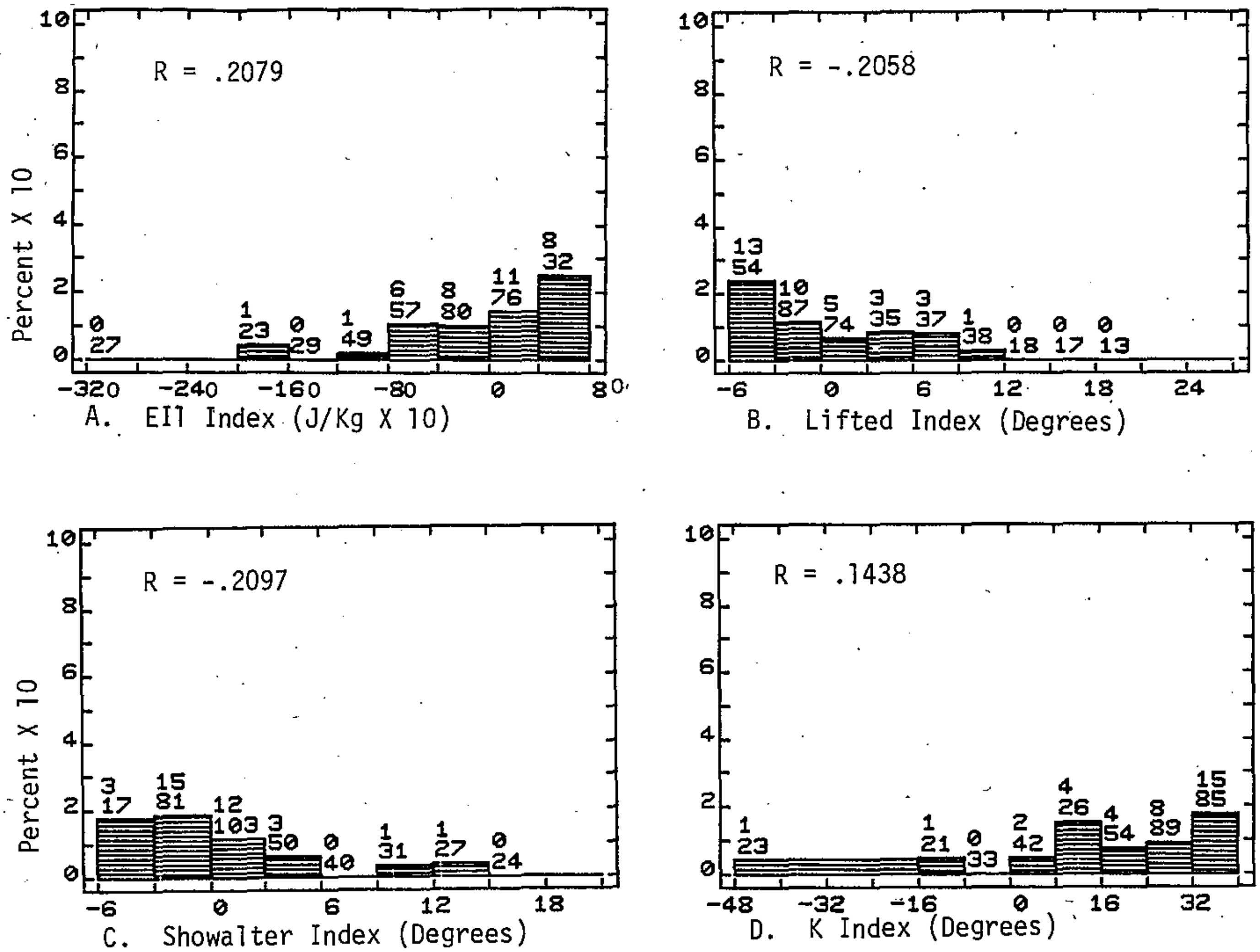

Fig. 3. Histograms of relative frequency of occurrence of severe weather (between 18Z-24Z) for various stability parameters computed from 1200 GMT raob data. Top number above each bar is number of severe weather occurrences; bottom number is total number of cases in the interval. Total number of cases is 373.

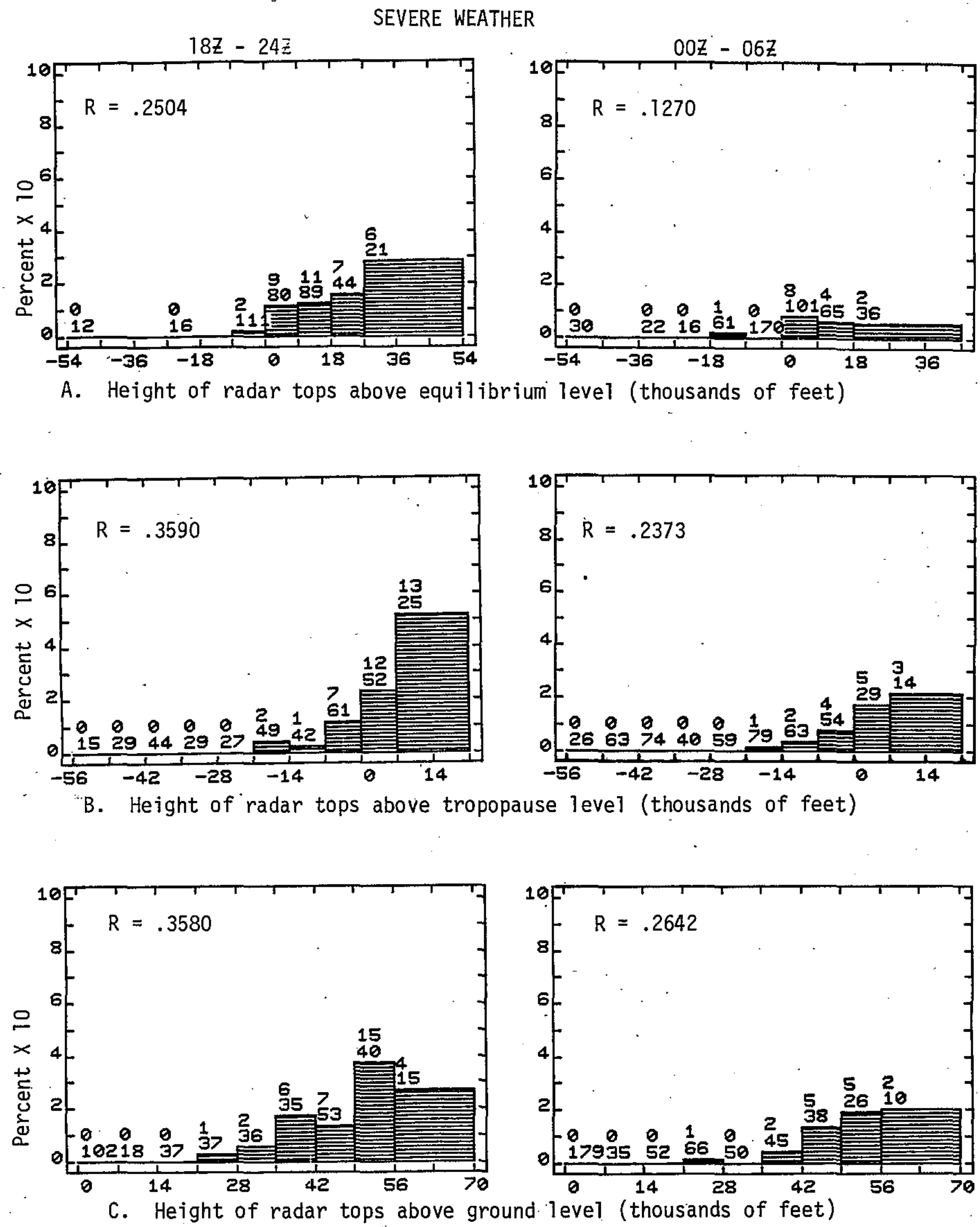

Fig. 4. Histograms of relative frequency of occurrence of severe weather for radar tops above various reference levels. Left side for time period 18Z-24Z (373 cases) and right side for 00Z-06Z (501 cases).